Final Draft
of the original manuscript:

Neffe, A.T.; Tronci, G.; Alteheld, A.; Lendlein, A.:

Controlled Change of Mechanical Properties during Hydrolytic Degradation of Polyester Urethane Networks

Full Paper

Controlled change of mechanical properties during hydrolytic degradation of polyester urethane networks [a]

Axel Thomas Neffe[b], Giuseppe Tronci[b], Armin Alteheld, and Andreas Lendlein*

_____

A. Lendlein, A.T. Neffe, G. Tronci
GKSS Centre for Biomaterial Development and Berlin-Brandenburg Centre for Regenerative Therapies (BCRT), Kantstrasse 55, 14513 Teltow, Germany, and University of Potsdam, 14476 Golm, Germany
Fax: +49-3328-352450; E-mail: andreas.lendlein@gkss.de

A. Alteheld
Present Address: BASF Venture Capital GmbH, 4. Gartenweg - Z25, 67063 Ludwigshafen, Germany

_____

Polyester urethane networks are versatile polymer systems as it is possible to tailor their mechanical properties and their hydrolytic degradation profile. For biomedical applications, the biodegradability as well as the thermomechanical properties of the polymer networks during the course of degradation is of importance. Therefore, we investigated the change of thermomechanical properties of networks based on star-shaped precursors of *rac*-dilactide and diglycolide, ε-caprolactone, or *p*-dioxanone, respectively, during hydrolytic degradation. Degradation rate and mechanical properties of the polymer networks were tailored by crosslink density, comonomers, and by changing the glass transition temperature. Most importantly, the degradation of the networks led to a controlled, step-by-step change of the mechanical properties of the networks.

---

[a] ⌨ Supporting information for this article is available at the bottom of the article's abstract page, which can be accessed from the journal's homepage at http://www.mrc-journal.de, or from the author. ((note: website is journal-specific))
[b] ATN and GT contributed equally to this work.

Introduction

Biodegradable polymeric materials are the basis for implants needed for a certain time only and for which a second surgery for removal of the implant should be avoided, such as controlled drug release implants,[1] internal sutures,[2] and applications in tissue engineering and induced autoregeneration.[3,4] Principally, biodegradable materials are based on the cleavage of certain bonds under physiological conditions. The cleavage itself can happen through hydrolysis (*e. g.* of ester bonds),[5,6] by enzymatic cleavage,[7] or miscellaneous mechanisms such as reduction of disulfide bonds,[8] and can be in the main- or side chains,[9] depending on the monomers and architecture of the polymer. In biodegradable materials, cleavage of the bonds results in water soluble polymer fragments, which can be excreted from the body, *e. g.* through the kidney.[10] The degradation process of the polymer materials can be observed on different levels, including mass loss, change of molecular weight, change of thermomechanical properties, and the occurrence of degradation products. Additionally to degradation studies of bulk material, hydrolytic and enzymatic degradation can also be studied on polymer monolayers.[11] The degradation rate can generally be adjusted by the types of monomers,[12] the sequence structure and architecture of the polymer,[13-16] as well as by the morphology. One of the first and most-widely used classes of biodegradable polymers are the bulk degrading polyesters such as PLGA, however many other degradable materials are known such as poly(anhydrides),[17] poly(orthoesters),[18] poly(depsipeptides),[19] and poly(ether esters).[20]

Semi-crystalline linear polyesters have been applied for sutures, for which mechanical stability is of high importance. One of the drawbacks of these semi-crystalline materials is their heterogeneous degradation profile resulting in changes of the crystallinity during the degradation and remaining fragments of insoluble and very slowly degrading material. By changing monomer types and ratios, also fully amorphous polyesters have been developed,

which have a more homogeneous degradation profile.[21] These have been applied for the design of degradable devices with complex geometry, however, water can easily act as softener in the amorphous matrix leading to reduced glass transition temperature, T_g, possibly influencing many properties including the diffusibility. Furthermore, the material integrity and mechanical properties of amorphous materials are connected to physical entanglements, which might disentangle under load leading to a relaxation of the material.[22] In any case, linear polyesters exhibit a high T_g, resulting in a tough glassy material, whereas some applications require more elastic materials.

One possibility to yield the required elasticity was the design of polymer networks. First of all, physically crosslinked polyester networks based on (multi)block copolymers have been designed,[23,24] and in a next step, chemically crosslinked materials have been introduced. In the latter case, crosslinking via acrylates and urethanes have found wide application.[25,26] Chemically crosslinked polymer networks can be tailored to have a high elasticity, which is *e. g.* required for specific functionalities of the network such as the shape-memory effect in general,[2, 27-31] and furthermore for multifunctional materials such as the recently described networks combining controlled drug release, biodegradability, and shape-memory.[32-35]

In biomedical applications, not only the mechanical properties at the beginning are of interest, but the course of biodegradation is of importance. For different applications, certain properties and their changes are of particular significance, e. g. the mass loss is vital for surface eroding drug release systems,[36,37] the mechanical stability at the beginning and during the course of the degradation is of interest for suture material,[38] types of fragments formed in the degradation have to be studied for the evaluation of the toxicity of materials and/or inflammatory responses to implanted materials,[39] and the change of diffusibility and the mass loss are crucial for diffusion controlled release systems.[40]

So far, mainly the mass loss over time has been studied. Albertsson and co-workers employed surface grafting techniques and monomer composition to enhance hydrophilicity of polyester-

based materials, such as substrates and networks, respectively.[40-43] Although both strategies enabled tailoring of degradation rate, the resulting materials were semi-crystalline, both in the intact and degraded form. As detailed above, these semi-crystalline materials potentially suffer from non-homogeneous degradation, due to the hindered diffusion of water molecules in the crystalline phase. With the aim of more homogeneous degrading amorphous materials,[44-48] Shen et al. synthesized photo-crosslinked, and only partially degradable, aliphatic polyesters acrylate networks via UV irradiation of linear poly[(ε-caprolactone)-*co*-lactide-*co*-glycolide] diacrylates.[49] The networks were completely amorphous and led to linear decrease of Young's modulus with degradation time, though sudden mass loss and rapid strain increase occurred in the degraded material. Following the same line of thinking, Amsden et al. investigated the degradation behaviour of amorphous elastomers deriving from photo-curing of three arms-shaped macromers, achieving controlled decrease of mechanical properties depending on the molecular weight of network precursors.[50,51]

As Amsden pointed out recently, especially the change of material properties over the time of degradation is crucial but not well studied.[52] Furthermore, the type of degradation products is important in biomedical applications. The change of mechanical properties of polyester based materials is only hard to predict, generally undergoing abrupt changes, which is problematic e. g. for degradable sutures. The formation of small fragments, which can behave totally differently in the body than the starting material, *e.g.* promoting immune or inflammatory responses, is a general concern for degradable polymers. Changes of properties such as degradation rate and diffusibility have to be taken into account for drug release systems and would best be avoided. Therefore, the challenge in ensuring clinical applicability of polymer materials based on biodegradable polyesters can only be overcome by predicting the rate of degradation, the change of the thermomechanical properties of the polymer matrix, as well as the occurrence of amount and type of fragments, while ensuring the full hydrolysis and/or

excretion of the polymer. To reach this goal, the degradation has to be understood as well on the molecular as on the macroscopic level.

For this purpose, the degradation of chemically crosslinked polyester urethane networks was studied in this work in detail. Networks resulting from crosslinking of star-shaped oligoester macrols with a mixture of 2,2,4- and 2,4,4-trimethylhexane-1,6-diisocyanate (TMDI) were varied in the number of netpoint arms, *i.e.* 3- and 4-armed netpoints. All networks were based on *rac*-dilactide copolymerized with diglycolide, ε-caprolactone, or *p*-dioxanone,[53,54] respectively, whereby the ratio of the comonomers and the segment length of the oligoester precursors were varied. All of the studied networks were fully amorphous. By the variation of the parameters of the networks, the thermal and mechanical properties of the networks were tailored. The glass transition temperature T_g of the networks at the beginning of the study was 14-66 °C. The mechanical properties of non-degraded networks as determined by tensile tests at 37 °C displayed Young's moduli E between 1.3 and 430 MPa, elongation at break ε_b between 40 – 580 %, and tensile strength σ_{max} between 1.5 and 24.9 MPa. For all of the networks, a shape-memory effect was demonstrated.[53,54]

In this work we wanted to address how thermal and mechanical properties of these polyester urethane networks change in the course of degradation, and which possibilities are available to ensure a homogeneous and predictable degradation, avoiding abrupt changes. By analyzing as well the partially degraded networks as the formed fragments, an understanding of changes of macroscopic properties and changes on the molecular level and a model for the course of degradation should be developed, aiming at controlling the rate of degradation and the changes of the networks properties during the degradation.

Experimental Part

Materials

rac-Dilactide (>96%, Sigma-Aldrich Chemie GmbH, Steinheim), diglycolide (Boehringer Ingelheim GmbH, Ingelheim), and 1,1,1-Tris(hydroxymethyl)ethane (Fluka Chemie AG, Neu Ulm; >98%) were recrystallized from ethylacetate. Pentaerythrole (>99%), 2,2,4- and 2,4,4-trimethylhexane-1,6-diisocyanate (>98%, TMDI) and dibutyltin oxide (DBTO) were used as received from Sigma-Aldrich Chemie GmbH. ε-Caprolactone (Sigma-Aldrich; 99%) was distilled over calcium hydride (Merck; ca. 95%). *p*-Dioxanone (Boehringer Ingelheim) was distilled under vacuum before use.

Synthesis of precursors

The synthesis has been described in detail before.[53,54] In brief, monomers and initiators were stirred under nitrogen at 130 °C. When the melt became optically clear, dibutyltin oxide (0.2 wt%) was added. After 5 days, the reaction mixture was cooled to room temperature. The *co*-oligomers were dissolved in a six- to ten-fold excess of CH_2Cl_2 and then precipitated in hexane.

Synthesis of copoly(ether)ester-urethane networks

The telechelic cooligomer was dissolved in a tenfold excess of CH_2Cl_2 under nitrogen. TMDI (in a molar ratio of isocyanate to hydroxy functional groups of 1.05) was added to the solution under stirring. After 5 min, the reaction mixture was poured into teflon dishes and kept under nitrogen flow for 24 h at room temperature to evaporate the solvent carefully during

formation of the polymer network. To complete the crosslinking, films were kept at 80 °C for further 4 days. The crude films were extracted with chloroform and dried to constant weight under vacuum (0.1 mbar) at 80 °C.

Hydrolysis experiments

Hydrolytic degradation of network films with the dimensions of 15 × 10 × 0.3 mm was investigated in PBS buffer containing 0.1 M Na_2HPO_4 and 63 mM KH_2PO_4 at pH 7.0 and 37 °C. Each film was placed in a centrifuge tube containing 15 mL of PBS. In order to avoid growth of microorganisms, sodium azide was added (250 mg $NaN_3 \cdot mL^{-1}$) to the degradation medium. At selected degradation time points, t_d, samples were taken out of the degradation medium and water uptake of the samples was determined as

$$H = \frac{m_s - m_d}{m_d} \tag{1}$$

where m_s is the wet mass of partially degraded bulk material, while m_d is the respective mass in the dry state, with either m_s or m_d referred to the selected degradation time point, t_d. Similarly, mass loss was calculated as follows:

$$\mu_{rel} = \frac{m_d}{m_0} \tag{2}$$

where m_0 is the initial dry mass of samples prior to hydrolytic degradation. After an initiation time, mass loss is following a pseudo-first order degradation as has been described before mathematically:[55]

$$\ln \frac{m(t)}{m_0} = A - kt \tag{3}$$

For the visualization in Figures 1-4, a linear regression analysis of the data points has been performed according to eq. 3 and a trendline helping the eye has been included into the plots using the values for A and k determined in the regression analysis.

After drying, thermal properties were investigated by Differential Scanning Calorimetry (DSC) on a Perkin Elmer DSC7 apparatus with low temperature cell equipped with a TA7 processor. During the first heating run, the samples were heated from 25 °C to 150 °C with a heating rate of 10 K·min^{-1}, kept at this temperature for two minutes and were cooled down to 0 °C with a cooling rate of 10 K·min^{-1}. In the second heating run, the samples were heated from 0 °C to 150 °C with a rate of 10 K·min^{-1}. Data from the second heating run was used for further analyses.

For tensile tests, the partially degraded bulk material test bodies were preconditioned for 4 h in water at 37 °C. Subsequently, the tensile tests were performed on three dumbbell-shaped replicas with 10 mm length, 3 mm width, and a thickness of 0.2 to 0.3 mm (determined by measuring) in water at 37 °C on a ZWICK1425 equipped with a thermo chamber (Climatic Systems LTD, model 091250) and a water bath of 2 L volume. The deformation rate was 10 mm·min^{-1} with an initial load of 30 mN·mm^{-2}.

Additionally, dried partially degraded bulk materials were extracted with chloroform for the determination of the gel content, G:

$$G = \frac{m_e}{m_d}$$

(4)

where m_e is the mass of extracted and dried samples at the selected degradation time point, t_d. The molecular weight and chemical composition of completely chloroform-soluble degradation products, i.e. either partially degraded networks or scission fragments, were investigated by Gel Permeation Chromatography (GPC) and ^{1}H-NMR. GPC was performed by serial usage of a T60A dual detector (differential viscosimetry and single angle (90°) light scattering detectors, Viscotek Corp., Houston, TX) and an optilab differential diffractometer (8721 ERC, Wyatt Technology, Santa Barbara, CA). The system was equipped with a mixed D column (600 mm×7.5 mm) and a LC1120 pump (Polymer Laboratories Ltd., Amherst, MA). Chloroform was used as eluent at a flow rate of 1.0 mL per minute. Universal

calibration was performed using narrow molecular weight distributed (MWD) polystyrene standards. Viscometric data and molecular weight calculation were performed with TriSEC GPC-Viscometry Module Software (Version 3.0, Viscotek Corp, Houston, TX).

^{1}H NMR-(400 MHz) spectra were recorded on a VARIAN INOVA 400 spectrometer in CDCl$_3$ or DMSO-d$_6$. Spectra were analyzed under the assumption that polymerization of monomers, leading to the synthesis of precursors, was initiated only by the hydroxyl functions of the initiator, and that only one initiator segment for each precursor, after polymerization, was present. Here, no distinction was considered about the exact chemical structure of component fragments formed during hydrolytic degradation, i.e. dimers, trimers, or oligomers. The time-dependent mass fraction, $\mu(t)$, was determined from the proton peaks of the specific sequences of polymer networks. Thus, mass fraction of each network component was normalized to the mass portion of the same component at the beginning of the experiment, μ_0, taking into account the change of relative mass, μ_{rel}.

Results and Discussion

Polyester urethane networks were synthesized by dibutyltin(II)oxide-catalyzed ring opening polymerization of *rac*-dilactide with a comonomer. *Rac*-dilactide is the racemic mixture of D,D-dilactide, L,L-dilactide, and *meso*-dilactide. The conomomers were diglycolide (LG networks), ε-caprolactone (LC networks), or *p*-dioxanone (LD networks), respectively, using 1,1,1-trishydroxymethylmethane (T) or pentaerythrite (P) as 3- or 4-armed initiators (structure see Supporting Information). Precursors with varying number average molecular weight M_n and comonomer ratios were then crosslinked using an isomeric mixture of 2,2,4- and 2,4,4-trimethylhexane-1,6-diisocyanate (TMDI), leading to the formation of networks with star-shaped netpoints.

Nomenclature used in this work for networks based on oligoester precursors is as follows: A-BB(XX)-YY with A = P or T, BB = LC, LD, or LG, XX = content of comonomer in the precursor in wt.-%, and YY = M_n of the precursors in kDa. The network based on 4-armed homopolymeric precursors of *rac*-dilactide was named P-L-10, where P and L refers to pentaerythrite and *rac*-dilactide, respectively, while 10 describes M_n of the precursors in kDa. M_n and conomomer content of the precursors were determined by integration of ^{1}H NMR spectra.

The bulk material was subjected to hydrolytic degradation in PBS buffer pH 7 at 37 °C. The mass loss, water uptake, and gel content of the test pieces were followed as macroscopic indicators of degradation. After drying, the thermal properties of the partially degraded networks were determined by DSC. In this way, changes of the molecular structure of the network during the degradation, such as formation of dangling chains or shift in monomer composition, should be monitored, some of which are likely to happen before a mass loss is evident. No endothermic peak was observed in resulting DSC thermograms of any studied network at any given time point, therefore the networks were completely amorphous during the whole time frame of the investigation. For the interpretation of the DSCs, the second heating run was used.

After resuspension in water, the mechanical properties of the networks were determined with tensile tests in the swollen state at 37 °C. The aim of this investigation was to see if abrupt changes in the mechanical properties would happen during the degradation or if a certain type of network composition and architecture could avoid this. Furthermore, it was of interest to see if a unidirectional change of E, σ_{max} and ε_b would occur or more complex changes of the mechanical properties would be observed. The change of mechanical properties during degradation could likewise be either due to a change of network molecular parameters or due to changes of T_g, as will be discussed by comparing thermal and mechanical properties. The remaining bulk material was subsequently treated with chloroform, leading to extraction of

chloroform soluble fragments from either P-LD or P-LC networks. Extracted fragments were then analyzed with ^{1}H-NMR spectroscopy. On the other hand, treatment with chloroform of LG networks resulted in completely soluble networks, allowing further analysis via GPC and ^{1}H-NMR spectroscopy (**Scheme 1**). In this way, the changes in network composition and the composition of the released fragments could be followed and analyzed. Thereby, a further insight into the degradation mechanism was gained.

P-LG networks with varying segment length and glycolide content

Figure 1 and **2** comprise the mass loss, water uptake, gel content, T_g, E, σ_{max}, and ε_b of the P-LG networks during the course of degradation, comparing networks with different segment lengths (precursor M_n = 1 to 10 kDa, 17 mol-% glycolide content, Figure 1) and glycolide content (precursor glycolide content 0-52 mol-%, M_n = 10 kDa, Figure 2). Trend lines fitting to pseudo first-order decay after a linear regression analysis according to eq. 3 have been added to the representation of the mass loss. Comparing networks with different segment lengths, mass loss was observed first for networks with a M_n of the precursors of 5000 g·mol^{-1} (after ca. 63 days), while networks with longer (M_n = 10000 g·mol^{-1}) and shorter (M_n = 1000 g·mol^{-1}) segment length showed mass loss much later (after 90 and 140 days, respectively). Likewise, water uptake H higher than 5 wt.-% was first observed in P-LG(15)-5 (after 50 days), followed by P-LG(17)-1 (after 70 days), and finally by P-LG(17)-10 (after more than 120 days). Changes in gel content G were observed in the same order. Comparing the networks with varying glycolide content, mass loss μ_{rel} was fastest for the networks with the highest glycolide content (starting to be observed after two weeks) and slowest for the homopolymeric lactide based systems (no mass loss observed within the first 180 days). Likewise, the increase of H was fastest for P-LG(52)-10 (50 wt.-% water uptake after two

weeks) and slowest for P-L-10 (5 wt.-% after 110 days). Also in this case, changes in G were observed in the same order as changes in μ_{rel} and H.

The T_g of the P-LG networks generally decreased with degradation time, which can be attributed to the increasing content of dangling chains during hydrolytic degradation. However, at certain time points a temporary increase of the T_g occurred as well, which is likely to be connected to a change in network composition, as will be discussed later in detail. Comparing networks with different segment lengths, the largest and fastest changes were observed for P-LG(17)-1 (from 63 to 30 °C after 180 days), and the changes were reduced and delayed with increasing M_n of the precursors. When comparing networks with different glycolide content, the increased glycolide content led to faster change of T_g, though the overall change till the end of the study was roughly similar for all the networks.

Tensile tests could be performed for the partially degraded P-LG(17)-10 networks up to 100 days of degradation, while for P-LG(17)-1 and P-LG(15)-5 these tests could not be performed anymore after roughly 60 and 50 days, respectively. The P-LG(52)-10 and P-LG(30)-10 networks could only be studied up to 10 and 20 days, respectively. This corresponds roughly to the time at which the water uptake into the networks exceeded 5 wt.-%, occurring before mass loss could be observed. E and σ_{max} were decreased with the time of degradation, though large differences from time point to time point and large variations between replicas were observed for network P-LG(17)-1. ε_b was constant or slightly increased, i. e. in the degrading network P-LG(17)-1, for at least 60 days, before an abrupt decrease was observed, e. g. in the degrading network P-LG(17)-10.

T-LG networks with varying segment length

Figure 3 comprises the mass loss, water uptake, gel content, T_g, E, σ_{max}, and ε_b of the T-LG networks during the course of degradation, comparing networks with different segment

lengths. Trend lines fitting to pseudo first-order decay after a linear regression analysis according to eq. 3 have been added to the representation of the mass loss.

The major difference to the P-LG networks discussed above was that the netpoints were 3-armed only. This change in network architecture had a tremendous influence on the degradation behaviour. Mass loss was observed first for networks with a M_n of the precursors of 1000 g·mol^{-1} (after ca. 50 days), and increased with increasing M_n of the precursors (T-LG(17)-5: start of mass loss after 70 days; T-LG(17)-10: start of mass loss after 80 days). Accordingly, water uptake H of more than 5 wt.-% was first observed in T-LG(17)-1 (after 20 days), followed nearly simultaneously by networks T-LG(17)-5 and T-LG(17)-10 (after roughly 40 days). Changes in the gel content were observed nearly at the same time for all T-LG networks starting after around 3 weeks of degradation.

The T_g of the T-LG networks generally decreased with degradation time, most notably for T-LG(17)-1 from 56 to 28 °C, while the changes in the networks from longer precursor were nearly the same (from 56 to 37 °C). Tensile tests could be performed for the partially degraded T-LG networks up to more than 40 days of hydrolytic degradation. This roughly corresponds to the time when the water uptake into the networks exceeded 15 wt.-%, occurring before mass loss could be observed. E and σ_{max} were decreased with the time of degradation, while ε_b first decreased, and than increased to values larger than the initial ones.

LC and LD networks with varying comonomer content

Figure 4 comprises the mass loss, water uptake, gel content, T_g, E, σ_{max}, and ε_b of the P-LC and LD networks during the course of degradation, comparing networks with different comonomer content. Trend lines fitting to pseudo first-order decay after a linear regression analysis according to eq. 3 have been added to the representation of the mass loss.

Mass loss was observed first for networks with higher ε-caprolactone content (21 mol-%, after 42 days), and then of the networks with lower ε-caprolactone content (12 mol-%, 63 days). Similarly, water uptake and decrease of gel content was observed earlier in the P-LC(21)-10 than in the P-LC(12)-10 networks. This finding is counterintuitive, as one would expect the more hydrophilic network to degrade faster.

The reason for this behaviour can be found when comparing the T_gs of these networks. The P-LC(21)-10 network had a T_g of 28 °C in the beginning of the experiment, which is already significantly lower than the temperature at which the degradation was performed. Therefore, the degradation was performed in the rubbery state on P-LC(21)-10 and in the glassy state on P-LC(12)-10. In the rubbery state, the diffusibility of the network is much higher, leading to a faster uptake of water and a faster loss of fragments. The change of T_g was also higher for P-LC(21)-10 than for P-LC(12)-10.

Likewise, mass loss was observed first for LD networks with higher p-dioxanone content (20 mol-%, after 42 days), and then of the networks with lower p-dioxanone content (12 mol-%, 49 days). Similarly, water uptake and decrease of gel content was observed earlier in the P-LD(20)-10 than in the P-LD(12)-10 networks. As in the case of the LC networks, the T_g of the P-LD networks was decreased with increasing p-dioxanone content, as result of the increased diffusibility.

Tensile tests could be performed on the partially degraded P-LC and P-LD networks up to almost 40 days of hydrolytic degradation. This roughly corresponds to the time when the water uptake into the networks exceeded 25 wt.-%, occurring before mass loss could be observed. E and σ_{max} were decreased during hydrolytic degradation. In the LC networks, ε_b was initially decreased, and then increased to values larger than the initial ones, as previously observed for T-LG networks. On the contrary, ε_b was steadily decreased during hydrolytic degradation of the LD networks.

Composition analysis of chloroform soluble networks and fragments

As demonstrated above, cleavage of single bonds in a network resulted in changes of the thermo-mechanical properties of the degrading network, as the crosslinking density and the architecture of the network are changed. However, after a certain degree of degradation, extractable fragments occur, and the investigation of the chemical composition of these fragments and of the remaining bulk network can offer an insight into the mechanism of degradation. Therefore, chloroform soluble networks were analyzed with ^{1}H-NMR. Starting from the proton peaks of the specific sequences in the spectrum of degrading networks, the change of mass fraction of each network component was calculated. The normalization of mass fractions at specific time points of degradation to the mass fraction at the beginning of the experiment, μ_0, under consideration of the change of relative mass, μ_{rel}, led to the determination of time-dependent mass fraction, $\mu(t)$, for each network component. Change of chemical composition of network P-LG(52)-10 during hydrolytic degradation is displayed as an example in **Figure 5**.

A decrease of glycolide content in the remaining network down to 30 wt.-% is observed during network degradation. The decrease in glycolide content of the remaining network during the degradation led simultaneously to an accumulation of lactide up to 60 wt.-% in the remaining network after 70 days of degradation. This change in network composition can be explained by the lower reactivity of lactate ester bonds to hydrolysis compared to glycolate ester bonds.

Apart from glycolide and lactide mass fractions, the content of pentaerythrite was almost constant, while the urethane content decreased during degradation but much slower compared to content of monomer and comonomer. This finding probably results from statistical considerations, as the cleavage of ester bonds and the following formation of degradation

products are less probable at the crosslinks compared to mid-chain cleavages in the polymer network.

Resulting changes of composition in network P-LG(52)-10 during degradation also explains the change of T_g in the degraded samples (Figure 2). First, the hydrolysis of single ester bonds resulted in enhanced water diffusion, while the following increase of T_g, on the other hand, can be connected to accumulation of sequences rich in lactide.

Based on ^{1}H-NMR results, Fox equation (5) for random copolymers was applied to network P-LG(52)-10, in order to calculate the expected T_g of the remaining sample:

$$T_g = w_1 \cdot T_{g1} + w_2 \cdot T_{g2} \tag{5}$$

where w_1 and w_2 are the respective fractions of monomer and comonomer, respectively, while T_{g1} and T_{g2} are the glass transition temperatures of the homopolymers, prepared from monomer and comonomer.

When using (1), as approximation the chloroform-soluble fragments were modelled as cooligomeric fragments. Thereby, presence of initiator and TMDI was completely neglected for the calculation of T_g of degrading material.

Figure 5b shows the comparison of experimentally and theoretically predicted change of T_g in degrading sample P-LG(52)-10. Fox equation describes rather well the increase of T_g in the second stage of degradation, though the T_g decrease at the beginning of degradation cannot be modelled, as it is not due to the change of network composition, but mainly to changes in material architecture.

Figure 6 depicts the loss of the different building blocks from the network P-LG(52)-10 over time. Glycolide units are lost first, followed by a nearly simultaneous loss of lactide and urethane linkers, while the pentaerythrite units are lost last.

The size of choroform-soluble fragments released from P-LG(30)-10 and P-LG(52)-10 networks was investigated by GPC (**Figure 7**). Soluble fragments appeared earlier in networks with increased glycolide content, suggesting hydrolytic cleavage of network chains starting at glycolate ester bonds. M_ws of fragments obtained at earliest time points were around 15 kDa and 16 kDa, in case of P-LG(30)-10 and P-LG(52)-10, respectively, and decreased to about 8 and 5 kDa, respectively, after almost 80 days of degradation. Correlating M_ws to the M_ns of the released fragments at different time points, it could be demonstrated that a shift in the polydispersity index (PI) of the fragments takes place. E.g.*,* the PI of the network P-LG(52)-10 was decreased from 8 to 5 during the degradation.

Additionally to the analysis described above, ^{1}H-NMR analysis of soluble fragments deriving from chloroform-extraction of either P-LD or P-LC networks was also carried out (**Figure 8**). In P-LD networks, similar change of chemical composition as in P-LG networks was observed. The decrease of comonomer content was strongly delayed compared to P-LG networks, with less than 10 wt.-% decrease in the content of *p*-dioxanone after 100 days of network degradation (Figure 8a). On the other hand, the fragments released from P-LC networks had higher lactide contents than the overall network, therefore, in the remaining network an increase in the content of *ε*-caprolactone occurred (Figure 8b). In the contrary, lactide content was increased in P-LG and P-LD networks. This behaviour is related to the hydrophilicity of the comonomer and susceptibility of the ester bonds to hydrolysis. Nevertheless, the absence of crystalline domains in the P-LC networks led to enhanced water diffusion compared to semi-crystalline homopolymers, promoting faster degradation of the P-LC networks than of the P-L-10 networks.

The ^{1}H-NMR analysis demonstrated that the increasing mass loss and water uptake, and decreasing gel content of the networks during hydrolytic degradation is connected to a change in network composition.

Discussion of the overall degradation mechanism

In the networks, the number of netpoint arms, monomer type and ratio in the precursors, and precursor segment length have been varied. All of these parameters have an influence on the degradation mechanism as observed for macroscopic properties of the partially degraded networks as well as on the molecular level.

The T-LG networks based on three-armed netpoints degraded faster than the P-LG networks based on four-armed netpoints. This was true for mass loss, water uptake, and changes of thermomechanical properties, and can at least partially be attributed to the decreased crosslink density. However, increasing segment length of the precursors did not lead to an increasing degradation rate, despite the lower crosslinking density. Likewise, changes of T_g were influenced by the M_n of the precursors, but no direct correlation was found. The reason is likely to be that two opposing effects connect degradation rate and segment length of the precursors. On the one hand, the segment length is inversely correlated to the crosslink density, as discussed above. On the other hand, in networks formed from precursors with low M_n, a higher content of urethane bonds is present and promotes the uptake of water despite the higher crosslinking density. Interestingly, the T-LG networks showed less influence of the segments lengths of the precursors on the degradation rate than the P-LG networks. Furthermore, the absolute and relative changes of the mechanical properties were less in the T-LG networks and the changes of Young's modulus were more uniform in the T-LG networks than in the comparable P-LG networks. The P-LG networks showed longer induction times but faster mass loss than T-LG networks.

Comparing networks with different comonomer content, the rate of degradation was only partially correlated with the content of the more hydrophilic and more easily hydrolyzed comonomer. In the LG networks, an increase in glycolide content corresponded to faster degradation. This was not the case for LC and LD networks, in which the more hydrophobic

networks degraded faster than the more hydrophilic networks. This highlights that the rate of degradation is connected to additional parameters one of which is the physical state of the polymer network during the degradation. All of the studied polymer networks were amorphous and glassy below T_g, however the hydrolysis experiments and tensile tests were performed at 37 °C, which was above T_g for some of the networks. In the rubbery state, the diffusibility is supposed to increase dramatically, leading to a faster uptake of water, hydrolysis of ester bonds, and fragment release from the degrading networks. Therefore, the degradation rate could be adjusted by changing the T_g of the networks.

While hydrolytic degradation is always connected to mass loss and water uptake, the changes of the thermomechanical properties of the polymer networks during the degradation help in the understanding of the degradation mechanism. The T_g of the networks was generally decreased, however, at certain time points a significant increase during the degradation was observed as well, most significantly for P-LG(17)-1 and all T-LG networks. The change of T_g generally can be connected to the number and lengths of dangling chains and to the monomer composition of the network. The change of T_g in all degrading networks was observed a long time before mass loss occurred, therefore T_g is a very sensitive indicator for the change of network architecture and composition. First, a decrease of T_g was found, which can be related to cleavage of bonds between netpoints, thereby increasing the number of dangling chains. The later increase of T_g in the networks however is connected to changes in the network composition which was monitored by ^{1}H NMR of chloroform soluble networks and fragments. In all cases, the more hydrophobic and simultaneously less hydrolyzed comonomer accumulated in the remaining network, which in turn led to a theoretically expected and found increase in T_g. The increase in T_g is displayed *e.g.* roughly after 80 days of degradation in sample T-LG(17)-1, and could be detected only after mass loss took place, occurring after ca. 50 days of degradation. E and σ_{max} values of all networks decrease during the course of degradation. These effects can be linked to the decrease of network density because of the

hydrolytic bond cleavages. The decrease of E was faster for networks with decreased M_n of the precursors, regardless of network architecture. This is somewhat surprising as these networks have a high crosslink density compared to the networks built from precursors with larger M_n. However, the increased TMDI content increased the hydrophilicity of the networks with low M_n of the precursors, which resulted in fast water uptake and start of the hydrolysis. Most interestingly, the change of ε_b differs from network to network. In some of the networks, ε_b was decreased constantly. In other networks, an increase of ε_b was observed. One possible explanation could be the physical entanglement of the formed fragments within the amorphous matrix. Hydrolysis, which occurred as it could be monitored by the changes in T_g and E, putatively led to the formation of fragments which are still to large to be released from the bulk (otherwise mass loss would be observed). The probably non-linear fragments can behave as strengthener.

Furthermore, the GPC analysis of the remaining chloroform soluble networks demonstrated a nearly exponential decrease of M_w which is more consistent with the release of larger star-shaped fragment than of smaller linear fragments.

The polyester urethanes showed a typical bulk degradation profile, i.e. the uptake and diffusion of water in the networks was considerably faster than mass loss. The cleavage of ester bonds in the network resulted in the presence of new carboxyl and hydroxyl functional groups in the network, enhancing the overall hydrophilicity of the network, and can in general act in autocatalytic fashion on further hydrolysis events. Additionally to the first cleavage, a backbiting of the free ends resulting in the formation of ring structures could principally occur, but has not been identified in the released fragments. In the further observation of T_g, a slight increase was observed after mass loss started. If the mass loss would have been because of the washing out of linear fragments, a further decrease of T_g would have been likely, as shorter chains have a lower T_g. Therefore, it is more likely that soluble star-shaped fragments are formed in the degradation.

Scheme 2 depicts the changes of the networks on a molecular level and correlates them to the macroscopic observations. (A) depicts the network directly after synthesis. After a small uptake of water (B), random hydrolysis leads to increased content of dangling chains in the network, thereby decreasing the network density as well as T_g and E. Subsequently, the rate of hydrolysis increases (C), however, the ester bonds which are cleaved predominantly belong to different chains, resulting in the formation of non-linear network fragments (D). The formation of these fragments can lead to an increase of ε_b due to entanglements of the dangling chains. The fragments are released from the network when small enough to be water soluble (E), which shifts network composition, leading to an increase in T_g. The last stage is the disintegration (F) of the network. The timeline for these steps depend on the initial composition and architecture of the network. Changes in the mechanical properties for some of the networks were connected to the tensile tests being performed at first below, and later above T_g, *i.e.* first in the glassy and later in the rubbery-like state.

The multi-step nature of the above mentioned degradation process also explains the wider variation on change of mechanical properties of P-LG and T-LG networks, based on multi-arm netpoints, compared to networks based on linear copolymers, thereby showing a nearly-linear decrease of mechanical properties differently to the literature described macrotriol-based networks.[47]

Conclusion

The detailed analysis of the thermomechanical properties and the molecular composition of amorphous polyester urethane networks over the course of hydrolytic degradation led to the understanding of the different steps in the degradation process of the networks on a molecular level, and how these steps are connected to the macroscopic effects. The steps which could be identified are uptake of water, initial bond cleavages, propagation of bond cleavages,

formation of non-linear fragments, release of soluble fragments, and finally disintegration of the network.

The T_g of the degrading networks is ruled by two opposing effects, i.e. the change of network architecture (leading to a decrease of T_g) and the change of network composition (here leading to an increase of T_g). The change of network composition starts much later than the change of architecture, leading to a wave-like changing of T_g. A similar, wave-like change was observed for ε_b in some networks, which was increased at certain time points, likely due to the formation of entangled non-linear fragments incorporated into the network. E decreased with the time in all studied networks, so that an abrupt loss of mechanical properties could be avoided, most notably in the low crosslinked T-LG networks. This is of particular importance as in this way the change of material properties can be predicted and takes place via incremental changes, raising confidence in their biomedical applicability. This paves the way in the approval of polymers as biomaterials for induced autoregeneration.

[1] P.R.J Gangadharam, S, Kailasam, D.R. Ashtekar, D.L. Wise, *J. Controlled Release* **1993**, *26*, 87.

[2] A. Lendlein, R. Langer, *Science* **2002**, *296*, 1673.

[3] P.A. Gunatillake, R. Adhikari, *Eur. Cell Mater.* **2003**, *5*, 1.

[4] T. Weigel , G. Schinkel, A. Lendlein, *Expert Rev. Med. Devices* **2006**, *3*, 835.

[5] D. Farrar, "Modelling of the degradation process for bioresorbable polymers", in: *Degradation Rate of Bioresorbable Materials*, F. Buchanan, Ed., Woodhead Publishing Ltd., Cambridge 2008, 183.

[6] C.-C. Chu, *Biomaterials* **2007**, 6/1.

[7] A.C. Albertsson, S. Karlsson, "Chemistry and biochemistry of polymer biodegradation", in: *Chem. Technol. Biodegrad. Polym.*, G.J.L. Griffin, Ed., Blackie, Glasgow 1994, 7.

[8] M. Breunig, U. Lungwitz, R. Liebl, A. Goepferich, *Proc. Natl. Acad. Sci. U.S.A.* **2007**, *104*, 14454.

[9] V. Lenaerts, P. Couvreur, D. Christiaens-Leyh, E. Joiris, M. Roland, B. Rollman, P. Speiser, *Biomaterials* **1984**, *5*, 65.

[10] A. Besheer, K. Mäder, S. Kaiser, J. Kressler, C. Weis, E.K. Odermatt, *J. Biomed. Mater. Res. B: Appl. Biomater.* **2007**, *82B*, 383.

[11]: A. Kulkarni, J. Reiche, K. Kratz, H. Kamusewitz, I.M. Sokolov, A. Lendlein, *Langmuir* **2007**, *23*, 12202.

[12] S.P.Valappil, S.K. Misra, A.R. Boccaccini, I. Roy, *Exp. Rev. Med. Dev.* **2006**, *3*, 853.

[13] R.M. Stayshich, J. Li, T.Y. Meyer, *Polymer Preprints* **2007**, *48*, 804.

[14] A. Lendlein, M. Colussi, P. Neuenschwander, U.W. Suter, *Macromol. Chem. Phys.* **2001**, *202*, 2702.

[15] A. Lendlein, P. Neuenschwander, U.W. Suter, *Macromol. Chem. Phys.* **1998**, *199*, 2785.

[16] M.Hakkarainen, G. Adamus, A. Hoglund, M. Kowalczuk, A.C. Albertsson, *Macromolecules* **2008**, *41*, 3547.

[17] N. Kumar, R.S. Langer, A.J. Domb, *Adv. Drug Deliv. Rev.* **2002**, *54*, 889.

[18] J. Heller, J. Barr, *Biomacromolecules* **2004**, *5*, 1625.

[19] Y. Feng, M. Behl, S. Kelch, A. Lendlein, *Macromol. Biosci.* **2009**, *9*, 45.

[20] H. Grablowitz, A. Lendlein, *J. Mater. Chem.* **2007**, *17*, 4050.

[21] D.A. Olson, S.E.A. Gratton, J.M. DeSimone, V.V. Sheares, *J. Am. Chem. Soc.* **2006**, *128*, 13625.

[22] P.G. Whitten, H.R. Brown, *Phys. Rev. E* **2007**, *76*, 026101.

[23] W. Wang, W. Wang, X. Chen, X. Jing, Z. Su, *J. Polym. Sci. B: Polym. Phys.* **2009**, *47* 685.

[24] P. Ping, W.S. Wang, X.S. Chen, X.B. Jing, *Biomacromolecules* **2005**, *6*, 587.

[25] S. Kelch, S. Steuer, A. M. Schmidt, A. Lendlein, *Biomacromolecules*, **2007**, 8, 1018.

[26] R.F. Storey, T.P. Hickey, *Polymer* **1994**, *35*, 830.

[27] A. Lendlein, S. Kelch, *Angew. Chem. Int. Ed*. **2002**, *41*, 2034.

[28] A. Lendlein, A. Schmidt, R. Langer, *Proc. Natl. Acad. Sci. USA* **2001**, *98*, 842.

[29] M. Bertmer, A. Burda, I. Blomenkamp-Höfges, S. Kelch, A. Lendlein, *Macromolecules* **2005**, *38*, 3793.

[30] D. Rickert, A. Lendlein, A. M. Schmidt, S. Kelch, W. Roehlke, R. Fuhrmann, R. P. Franke, *J. Biomed. Mater. Res*. **2003**, *67*, 722.

[31] N.-Y. Choi, S. Kelch, A. Lendlein, *Adv. Eng. Mat.* **2006**, *8*, 439.

[32] A. T. Neffe, B.D. Hanh, S. Steuer, A. Lendlein, *Adv. Mater.* **2009**, *21*, 3394.

[33] C. Wischke, A.T. Neffe, S. Steuer, A. Lendlein, *J. Controlled Release* **2009**, *138*, 243.

[34] A.T. Neffe, B. D. Hanh, S. Steuer, C. Wischke, A. Lendlein, "Thermomechanical Properties and Shape-Memory Capability of Drug Loaded Semi-Crystalline Polyestermethacrylate Networks", in: *Active Polymers*, A. Lendlein, V. Prasad Shastri, K. Gall, Eds., Mater. Res. Soc. Symp. Proc. Volume 1190, Warrendale 2009, in press, 1190-NN06-02

[35] C. Wischke, A.T. Neffe, S. Steuer, A. Lendlein, „Amorphous polymer networks combining three functionalities: shape-memory, biodegradability, and drug release", in: *Active Polymers*, A. Lendlein, V. Prasad Shastri, Ken Gall, Eds., Mater. Res. Soc. Symp. Proc. Volume 1190, Warrendale 2009, 1190-NN11-34.

[36] J. Heller, *J. Controlled Release* **1985**, *2*, 167.

[37] K.C.Wood, H.F. Chuang, D.M. Lynn, P.T. Hammond, *PMSE Preprints* **2005**, *93*, 281.

[38] T. Nilsson, Scand. *J. Plastic Reconstr. Surg.* **1982**, *16*, 11.

[39] P.Y. Wang, J. Biomed. *Mater. Res*. **1989**, *23*, 91.

[40] K.E. Uhrich, S.M. Cannizzaro, R.S. Langer, K.M. Shakesheff, *Chem. Rev.* **1999**, *99*, 3181.

[41] M. Hakkarainen, A. Höglund, K. Odelius, A.C. Albertsson, *J. Am. Chem. Soc.* **2007**, *129*, 6308.

[42] A. Höglund, K. Odelius, M. Hakkarainen, A.C. Albertsson, *Biomacromolecules* **2007**, *8*, 2025.

[43] M. Källrot, U. Edlund, A.C. Albertsson, *Biomacromolecules* **2007**, *8*, 2492.

[44] S. Li, J. Biomed. *Mater. Res.* **1999**, *48*, 342

[45] I. Jabbal-Gill,W. Lin, O. Kistner, S. S. Davis, L. Illum, *Adv. Drug Delivery Rev*. **2001**, *51*, 97.

[46] C. Witschi, E. Doelker, *J. Controlled Release* **1998**, *51*, 327.

[47] E. R. Edelman, A. Nathan, M. Katada, J. Gates, M. J. Karnovsky, *Biomaterials* **2000**, *21*, 2279.

[48] M. Ramchandani, D. Robinson, *J. Controlled Release* **1998**, *54*, 167.

[49] J.Y. Shen, X.Y. Pan, C.H. Lim, M.B. Chan-Park, X. Zhu, R.W. Beuerman, *Biomacromolecules* **2007**, *8*, 376.

[50] B.G. Amsden, G. Misra, F. Gu, H. M. Younes, *Biomacromolecules* **2004**, *5*, 2479.

[51] B.G. Amsden, M.Y. Tse, N.D. Turner, D.K. Knight, S.C. Pang, *Biomacromolecules* **2006**, *7*, 365.

[52] B. Amsden, *Soft Matter* **2007**, *3*, 1335.

[53] A. Alteheld, Y. Feng, S. Kelch, A. Lendlein, *Angew. Chemie Int. Ed.* **2005**, *44*, 1188.

[54] A. Lendlein, J. Zotzmann, Y. Feng, A. Alteheld, S. Kelch, *Biomacromolecules* **2009**, *10*, 975.

[55] R.A. Kenley, M. Ott Lee, T.R. Mahoney, L.M. Sanders, *Macromolecules* **1987**, *20*, 2398.
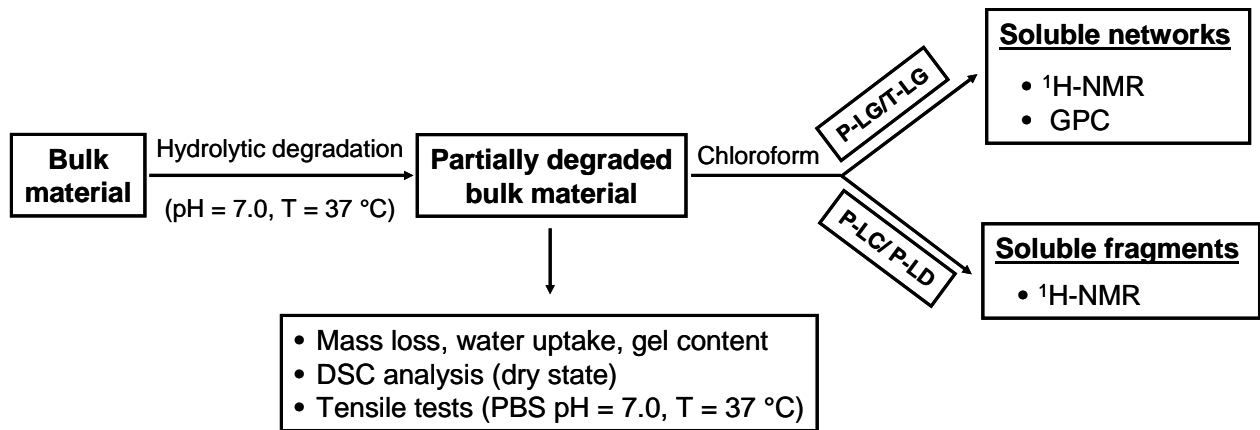
Scheme 1. Overview of material characterization carried out during hydrolytic degradation on either remaining bulk or on chloroform-treated material.
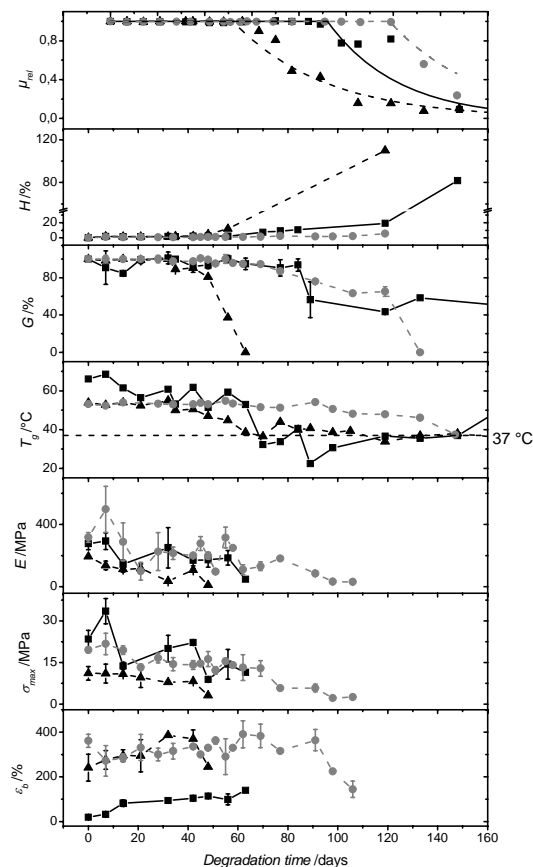
Figure 1. Change of material properties during hydrolytic degradation of macrotetrol-based P-LG networks differing in segment length. From top to bottom: mass loss (incl. trend lines according to eq. 3), μ_{rel}; water uptake, H; gel content, G; glass transition temperature, T_g; Young's modulus, E; maximal tensile stress, σ_{max}; elongation at break, ε_b. (— and ■) P-LG(17)-1, (-- and ▲) P-LG(15)-5, (-- and ●) P-LG(17)-10.
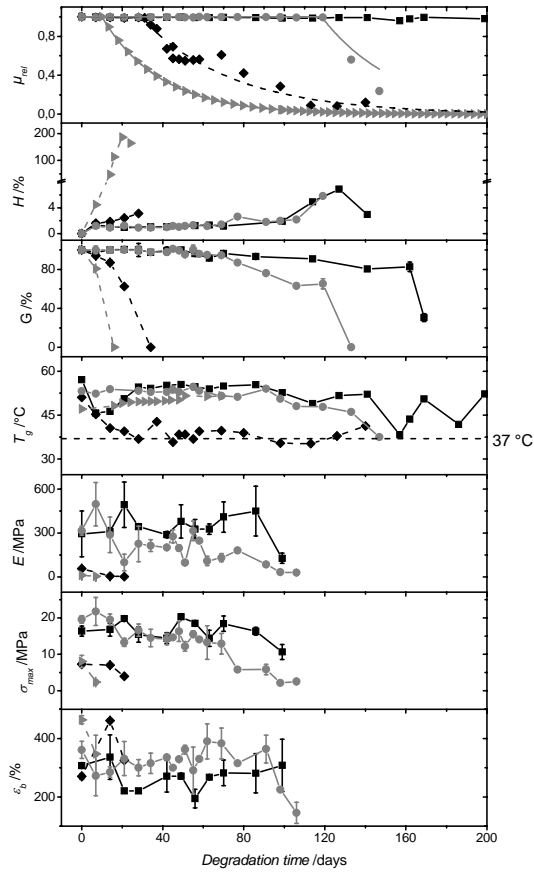
Figure 2. Change of material properties during hydrolytic degradation of macrotetrol-based P-LG networks differing in glycolide content. From top to bottom: mass loss (incl. trend lines according to eq. 3), μ_{rel}; water uptake, H; gel content, G; glass transition temperature, T_g; Young's modulus, E; maximal tensile stress, σ_{max}; elongation at break, ε_b . (—— and ■) P-L-10, (—— and ●) P-LG(17)-10, (-- and ♦) P-LG(30)-10, (-- and ►) P-LG(52)-10.
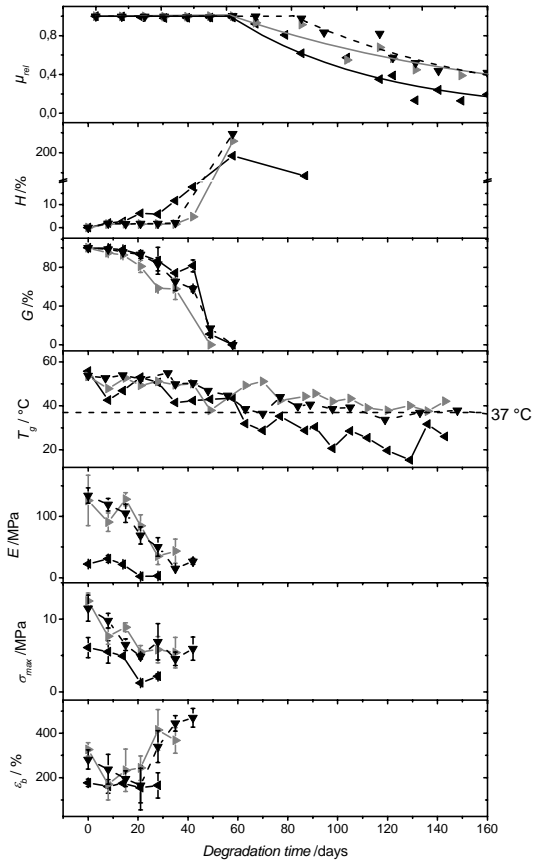
Figure 3. Change of material properties during hydrolytic degradation of macrotriol-based T-LG networks. From top to bottom: mass loss (incl. trend lines according to eq. 3), μ_{rel}; water uptake, *H*; gel content, *G*; glass transition temperature, T_g; Young's modulus, *E*; maximal tensile stress, σ_{max}; elongation at break, ε_b . (— and ◄) T-LG(17)-1, (-- and ▼) T-LG(15)-5, (— and ►) T-LG(17)-7.
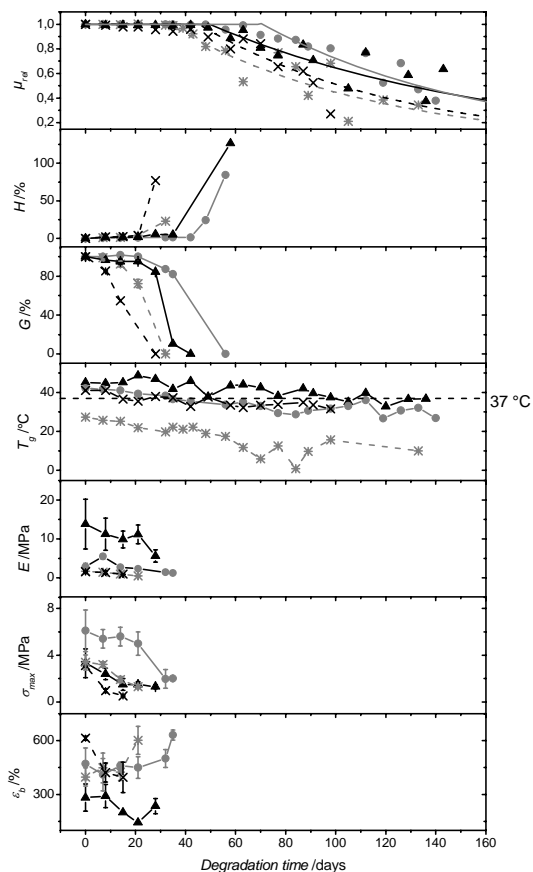
Figure 4. Change of material properties during hydrolytic degradation of macrotetrol-based P-LC and P-LD networks. From top to bottom: mass loss (incl. trend lines according to eq. 3), μ_{rel}; water uptake, H; gel content, G; glass transition temperature, T_g; Young's modulus, E; maximal tensile stress, σ_{max}; elongation at break, ε_b. (-- and ×) P-LD(20)-10, (— and ▲) P-LD(12)-10, (-- and *) P-LC(21)-10, (— and ●) P-LC(12)-10.

A   B
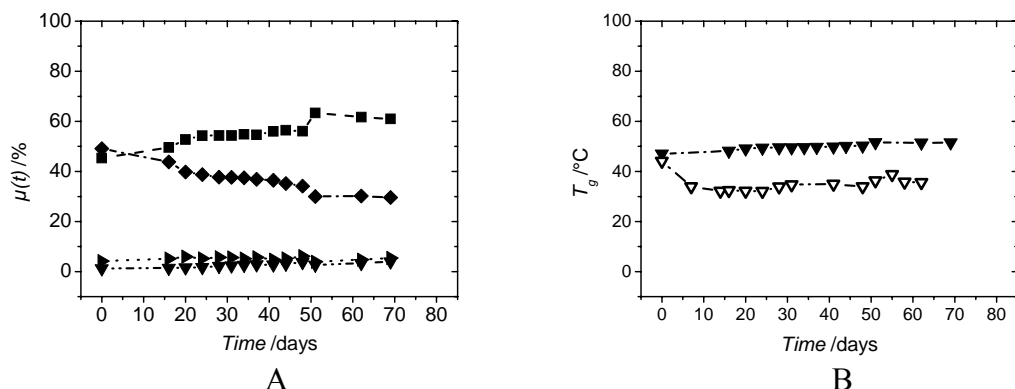
Figure 5. (A) change of chemical composition assessed by ^{1}H-NMR of network P-LG(52)-10 during hydrolytic degradation. (--■--): lactide, (·-·♦·-·): glycolide, (···▶···): urethane, (·-··▼··-·): pentaerythrite. (B): change of glass transition temperature (T_g) during degradation of network P-LG(52)-10 determined experimentally (---▽---) and predicted theoretically by the Fox equation (---▼---), starting by the mass fractions of lactide and glycolide as assessed by ^{1}H-NMR.
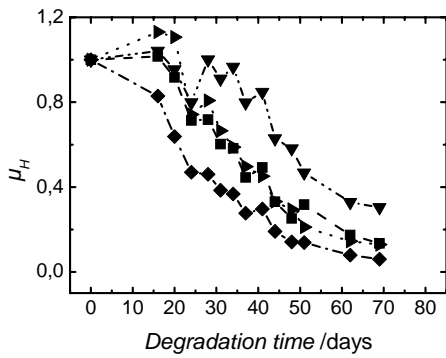
Figure 6. Change of mass fraction, μ_H, of lactide (—■—), glycolide (——◆——), pentaerythrite (····▲····), and urethane (—·—▼—·—), during hydrolytic degradation of P-LG(52)-10.
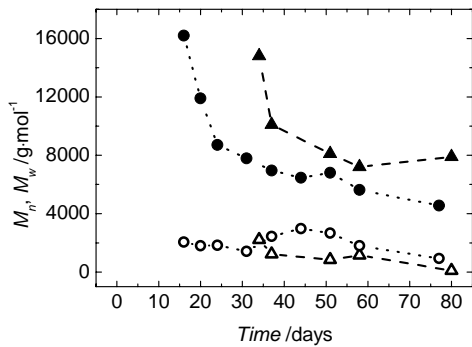

Figure 7. Change of molecular weight assessed by GPC of chloroform-soluble fragments during hydrolytic degradation of either network P-LG(52)-10 (--•-- M_w, --○-- M_n) or network P-LG(30)-10 (--▲-- M_w, --△--M_n).
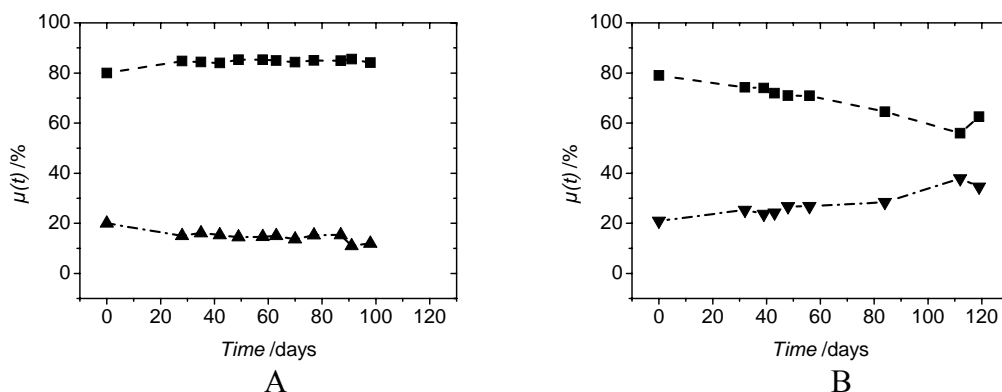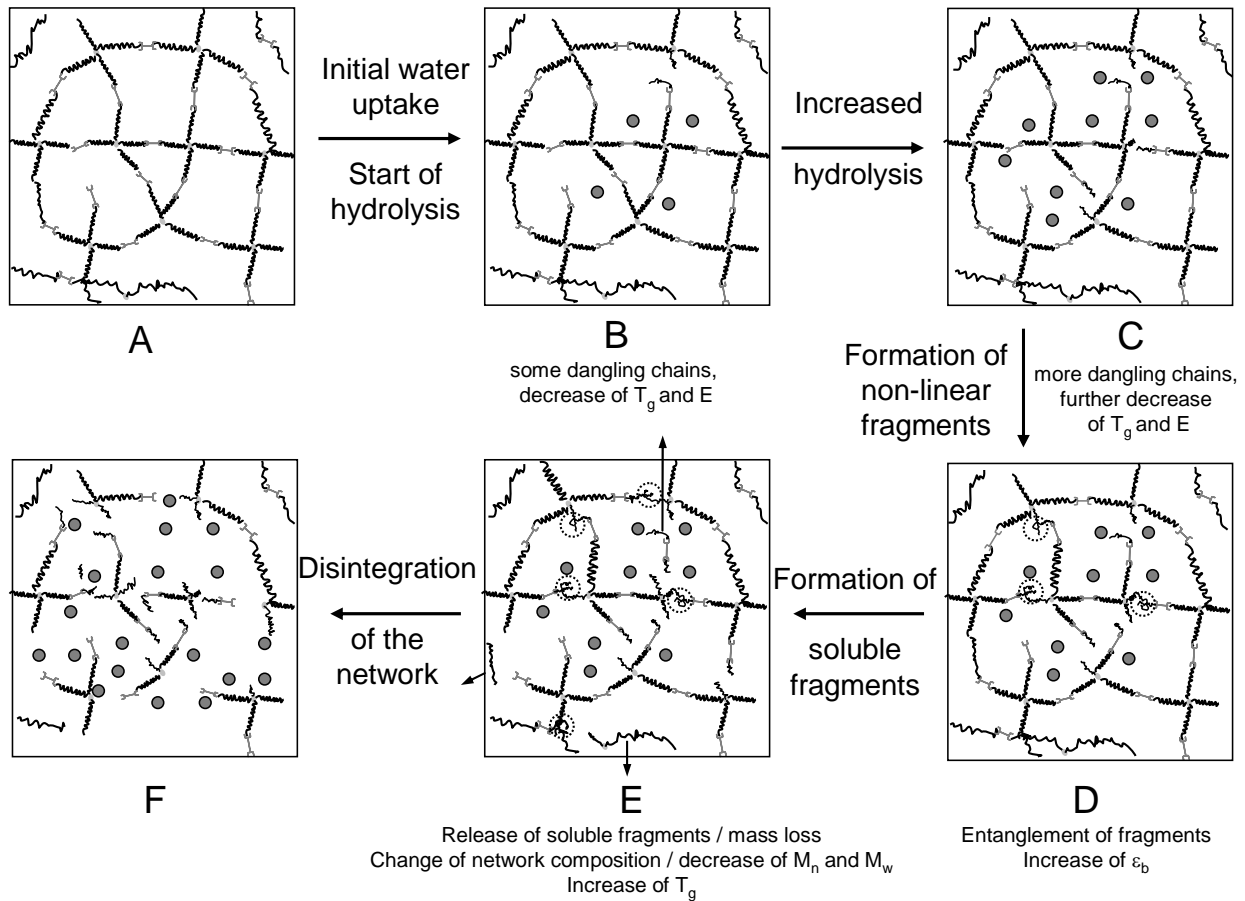


A   B

Figure 8. Change of chemical composition assessed by ^{1}H-NMR of either network P-LD(20)-10 (A) or network P-LC(21)-10 (B) during hydrolytic degradation. (--■--): Lactide, (--▲--): *p*-dioxanone, (--▼--): *ε*-caprolactone.

*Scheme 2.*Molecular changes of polyester urethane network during hydrolytic degradation. A) Initial network. B) Uptake of a small amount of water (●) leads to first bond clevages. C) Subsequently, increased hydrolysis, production of further dangling chains and decrease of T_g of the network is observed. D) Entanglement (◌) of non-linear fragments formed by random cleavage of ester bonds on different chains with remaining parts of the network has a strengthener effect, resulting in an increase ε_b. E) Further bond cleavages result in the formation of soluble fragments, leading to mass loss and change of network composition. F) Finally, the network disintegrates.
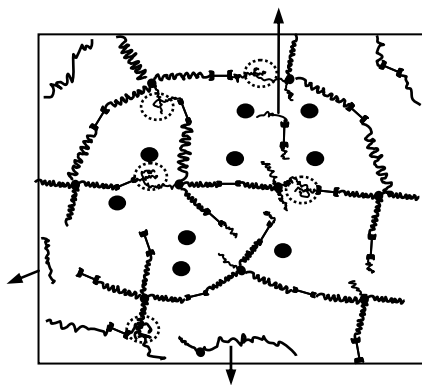
Graphic for the abstract

Full Paper

The changes of thermomechanical properties of amorphous polyester urethane networks with tailored mechanical properties and degradation rate during hydrolysis are connected to changes of the networks on the molecular level. The formation of entangled non-linear fragments (Scheme) within the degrading networks lead to an increase of elongation at break of the degrading networks and to a step-by-step reduction of the E modulus, so that an abrupt change of mechanical properties can be avoided.
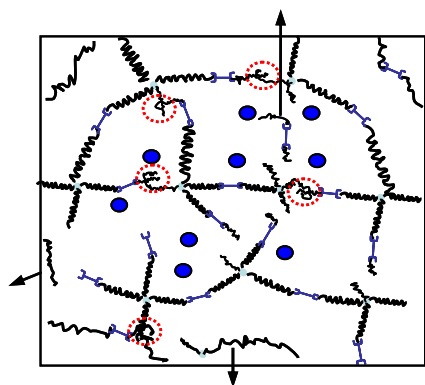

A.T. Neffe, G. Tronci, A. Alteheld, A. Lendlein*

Controlled change of mechanical properties during hydrolytic degradation of polyester urethane networks

Supporting Information for

"**Controlled change of mechanical properties during hydrolytic degradation of polyester urethane networks**"

By Axel T. Neffe, Giuseppe Tronci, Armin Alteheld, and Andreas Lendlein*

I = *neo*-pentyl (x= 4), CH(CH₂)₃ (x = 3)
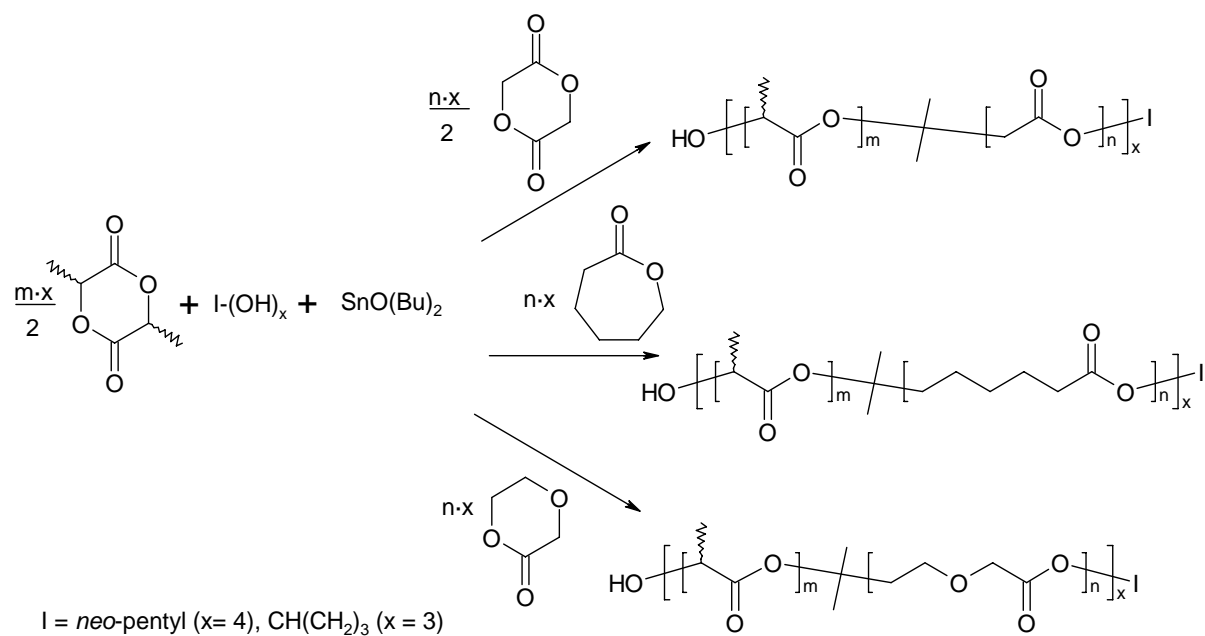
Scheme 1. Synthesis and structure of network precursors